Hexagonal-Columnar Mesophases in Substituted Phthalocyaninatopolysiloxanes

Thomas Sauer†

Max-Planck-Institut für Polymerforschung, Postfach 3148, 6500 Mainz, FRG

Received August 5, 1992; Revised Manuscript Received January 12, 1993

ABSTRACT: The study of the phase behavior of alkoxy-substituted phthalocyaninatopolysiloxanes reveals the existence of three different classes of this type of polymer, depending on the side chain length. Short side chain derivatives do not show any phase transition up to the decomposition temperature. Medium side chain derivatives show a transition to a highly viscous liquid-crystalline phase while the long side chain derivatives have an additional fluid mesophase at higher temperatures. In all solid and liquid-crystalline phases the rodlike molecules are packed in a two-dimensional hexagonal lattice with no discontinuous structural variations at the phase transition temperatures. This type of molecular packing is called the hexagonal-columnar phase. Its high thermal stability is a consequence of the cylindrical symmetry and the very high chain stiffness of the polymers under investigation. Short side chains are in a disordered state characterized by a low-temperature glass transition. Longer side chains tend to partially crystallize in a hexagonal sublattice at room temperature. About ten methylene units are necessary to decouple crystallizing side chain segments from the polymer main chain. The free volume of the side chain segments in the liquid-crystalline state has been determined experimentally from the X-ray scattering data of a homologous series of side chain lengths to be about 20% of the hard core volume. The thermal stability of these polymers is limited by side chain cleavage which is taking place in the range 250–300 °C. The assumed cleavage mechanism is pyrolysis via β-elimination rather than oxidation.

Introduction

Extensive research efforts on the synthesis and characterization of rodlike macromolecular systems modified with flexible side chains have led to a variety of polymeric materials which are quite intractable without those substituents.[1] The additional degrees of freedom of the flexible substituents drastically enhance the solubility of these polymers in a variety of common organic solvents because of entropic reasons, while the corresponding unsubstituted materials are only soluble in quite aggressive media. Moreover large melting point depressions are observed due to the same reasons.

We recently reported on high molecular weight phthalocyaninatopolysiloxanes decorated with flexible alkoxy side chains.[2] The molecular structure of these polymers is shown in Figure 1. Using improved synthetic procedures these polymers were obtained in high yields under very moderate conditions.[3] Due to the very good solubility of these materials in a variety of organic solvents, we were able to determine the molecular weights on an absolute scale by scattering experiments from dilute solutions.[2,4] Furthermore the rigid rod nature of these macromolecules has been proofed by the angular dependence of the experimental scattering function, indicating that these macromolecules have the overall shape of rigid, circular cylinders. This finding is of course different from other rodlike polymers with flexible side chains, namely fully aromatic polyesters, polyamides, and polyimides. These polymers have been demonstrated as adopting a more plate- or ribbonlike molecular conformation in the bulk.[5] Also the wormlike chain model seems to describe the single molecule conformation of these species more accurately by taking into account the intrinsic main chain flexibility due to bond angle fluctuations out of the projected direction of the molecular long axis.[6] The single chain conformations of these polymers are still under debate because experimental determination in dilute solution is complicated by aggregation phenomena. The platelike structure of the repeat units allows for intermolecular aggregation due to attractive π-electron interactions. This situation is quite different in our system since the aromatic phthalocyanine rings are completely imbedded in a shell of aliphatic side chains. This is assumed to be the major reason for the fact that in this case no aggregation phenomena are observed in dilute solution.[4] It is anticipated that these differences in molecular architecture also influence the phase behavior in the bulk.

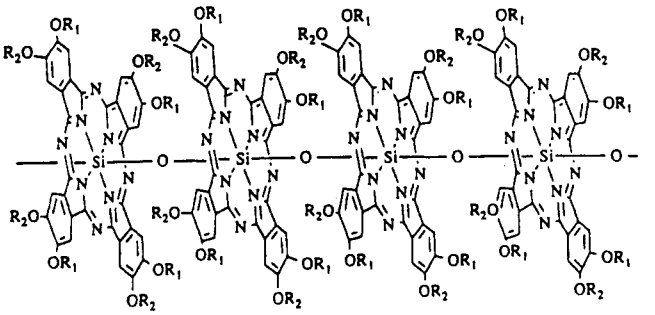

CnPCPS $R_1 = R_2 = C_nH_{2n+1}$

$n = 6, 8, 10, 12, 16, 18$

C1C8PCPS $R_1 = CH_3$; $R_2 = C_8H_{17}$

Figure 1. Molecular structure of alkoxy-substituted phthalocyaninatopolysiloxanes. Abbreviations are indicated for the different side chain derivatives used throughout the text.

Due to the fact that the substituted phthalocyaninatopolysiloxanes have an anisotropic rigid rod conformation with typical axial ratios in the range 6–15[4] these polymers have the potential to form thermotropic liquid-crystalline phases. As we have demonstrated in previous work,[2-4] the introduction of the alkoxy side chains leads to excellent solubility in common organic solvents. At the same time this substitution pattern leads to a considerable melting point depression compared to the nonfusible, unsubsti-

† Permanent address: Hüls AG, UB2 FE43, Postfach 1320, 4370 Marl, FRG.

0024-9297/93/2226-2057$04.00/0

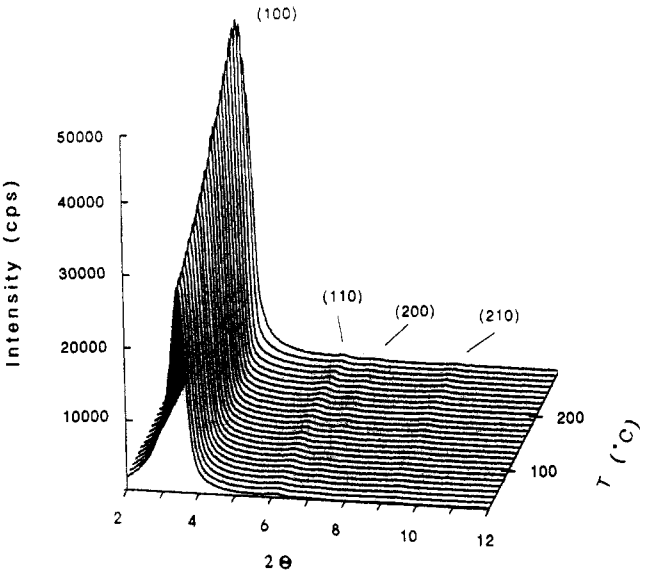

Figure 2. Temperature dependence of the powder X-ray diffraction pattern of C8PCPS. Numbers in parentheses denote Miller indices.

tuted phthalocyaninatopolysiloxane.[7] In this paper we report on our investigations on the thermal properties of substituted phthalocyaninatopolysiloxanes, namely the phase behavior in the bulk with respect to the molecular conformation already known from scattering experiments in dilute solution.[4] Moreover some results on the thermal stability of these polymers are presented.

Experimental Section

The synthesis of alkoxy-substituted phthalocyaninatopolysiloxanes and their characterization in dilute solution has been reported in detail elsewhere.[2-4] All samples were purified by repeated precipitation and subsequent freeze-drying from benzene solution. All spectral and elemental analysis data were in accordance with the assigned structure.

Optical textures were observed using a Zeiss photomicroscope III with a Mettler Thermosystem FP800 or a Linkam Scientific Instruments TH600 hotstage. DSC measurements were carried out on a Mettler DSC TA3000 and a Perkin-Elmer DSC 7. Usually, heating/cooling rates of 10 °C/min were used. X-ray measurements were carried out on nonoriented powder samples in the reflection mode using a Siemens D500 diffractometer (monochromatic Cu Kα radiation) together with a TTK hotstage from Anton Paar KG having an accuracy of ±0.5 °C. Samples were heated to the temperature of measurement several minutes before taking the actual diffraction pattern. Additionally, scattering patterns in the transmission mode were obtained with a flat camera equipped with a hotstage using Ni-filtered Cu Kα radiation. Thermogravimetric analysis (TGA) and differential thermogravimetric analysis (DTA) were carried out on a Mettler TG50 instrument. Infrared spectra were obtained from KBr pellets using a Nicolet SX60 FTIR spectrometer.

Results

Phase Behavior. Due to their thermal properties the alkoxy-substituted phthalocyaninatopolysiloxanes can be divided into three classes of materials according to their side chain length (see Figure 1).

1. Short Side Chains (R = C_6H_{13}, C_8H_{17}, C_8H_{17}/CH_3). These materials do not show any observable phase transition upon heating to the decomposition temperature of the alkoxy side chains, which is in the range of 300 °C and which will be discussed in detail below. Over this whole temperature range the polymers are in a solid modification, the powder X-ray diffraction pattern of which is shown in Figure 2 as a function of temperature. For all samples a very intense small-angle diffraction peak together with a number of higher order reflections is obtained. This pattern can be indexed in a two-dimensional hexagonal lattice according to

$$d(h,k,0) = 1/\sqrt{\frac{4}{3D^2}(h^2 + hk + k^2)} \qquad (1)$$

Here d is the experimental value of the Bragg spacing, h and k are the Miller indices in two dimensions, and D is the rod diameter. In comparison to the smectic B phase which has the same lateral packing, there is no periodic ordering of the centers of gravity of the macromolecules along the molecular long axis. Of course such a feature is not expected because of the considerable polydispersity of the polymer samples, which is of the order of $M_w/M_n = 2$.[4] The arrangement of monomer units along the single polymer backbone, which is the only register in the c direction, should not give rise to any intermolecular correlation. The absence of positional correlation in this direction, however, does not imply that there is a reduced dimensionality of molecular orientational distribution which is found experimentally in Langmuir–Blodgett films from C1C8PCPS.[8]

The same type of diffraction pattern is found from all derivatives comprising this group of polymers, and actual data are summarized in Table I. From the scattering pattern the diameter of an equivalent homogeneous cylinder corresponding to the rodlike particles can be calculated by

$$D = \sqrt{\frac{4}{3}}d(100) \qquad (2)$$

The increase in peak intensity and the decrease in line width with increasing temperature is a clear sign for a thermal annealing process which leads to an increase in orientational order (see Figure 9). The wide-angle region of the diffraction curves shows a relatively sharp peak around 3.4 Å, which is assigned to the periodic arrangement of monomer units along the main chain (Figure 3). This parameter shows a systematic increase with the side chain length which is due to steric hindrance by the increasing volume fraction of the side chains. Data for the different compounds are found in Table II. At a Bragg spacing of about 4.5 Å the amorphous halo from the disordered side chains appears. The corresponding glass transition temperature is found by DSC measurements at about −55 °C with a Δc_p of about 0.2 J g^{-1} K^{-1}.

An interesting feature is found from the temperature dependence of the lattice parameters of the unsymmetrically substituted C1C8PCPS. While other derivatives show a linear increase of the d spacings due to thermal expansion, C1C8PCPS, as obtained by synthesis, shows a remarkable decrease in the $d(100)$ spacing (and corresponding higher order reflections) up to 100 °C upon the first heating cycle (Figure 4). Above this temperature a linear increase due to thermal expansion is observed. Upon cooling, the system follows the linear relationship down to room temperature. The thermal expansion coefficient is in the range 0.8×10^{-4} K^{-1}, also for all other polymers under investigation.

This feature can be attributed to the particular substitution pattern of this polymer. The solvent-cast sample shows a lower density due to high disorder and low packing density in the side chain region. The effective molecular diameter is governed by the longer of both side chains. Thermal annealing leads to a much denser packing, as shown schematically in Figure 4 where the cross-section of the rigid rod macromolecules is dominated equally by both types of side chains. The polymer behaves as having

Table I
Bragg Spacings (in Å, Measured at 100 °C) of Substituted Phthalocyaninatopolysiloxanes As Obtained by Powder X-ray Diffraction and Their Indexing in a Two-Dimensional Hexagonal Lattice

(hk0)	C1C8PCPS	C6PCPS	C8PCPS	C10PCPS	C12PCPS	C16PCPS	C18PCPS
(100)	22.49	24.16	25.27	30.62	31.42	35.70	36.50
(110)	12.86	13.85	14.67	17.50	18.13	20.70	20.95
(200)	11.19	11.95	12.76	15.10	15.86	17.84	18.15
(210)	8.45	8.99	9.51	11.35	11.96	13.59	13.89
(300)		7.92			10.40		
(220)					9.12		
(310)		6.59			8.66		
(400)					7.84		

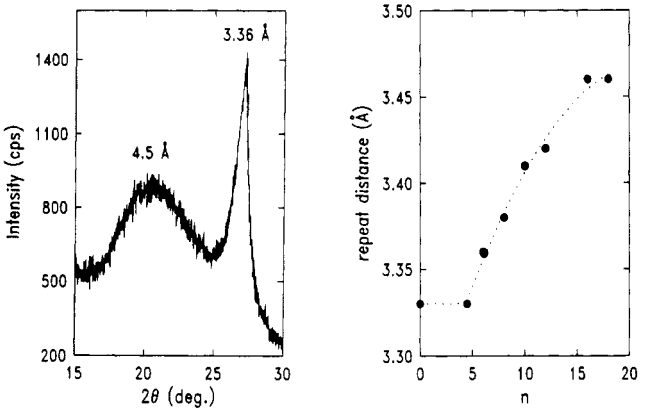

Figure 3. Wide-angle X-ray diffraction pattern of C6PCPS at room temperature (left) and the variation of the intramolecular repeat distance with the side chain length (right).

Table II
X-ray Data of Alkoxy-Substituted Phthalocyaninatopolysiloxanes As Obtained by Powder X-ray Diffraction (at 100 °C) and Quantities Calculated Thereof

polymer	d(100) (Å)	repeat dist (Å)	rod diam (Å)	cross section (Å²)	density (g cm⁻³)
C1C8PCPS	22.49	3.33	25.97	529.7	1.12
C6PCPS	24.16	3.36	27.90	611.3	1.10
C8PCPS	25.27	3.38	29.18	668.7	1.15
C10PCPS	30.62	3.41	35.36	981.8	0.89
C12PCPS	31.42	3.42	36.28	1033.8	0.95
C16PCPS	35.70	3.46	41.22	1334.6	0.89
C18PCPS	36.50	3.46	42.15	1395.1	0.93

a mean side chain length of 4.5 carbon atoms. This structural modification is then stable upon subsequent heating and cooling. The mass density of the original structure at 30 °C is calculated to be ρ = 1.08 g cm^{-3} according to X-ray data, while the annealed modification has an X-ray density of ρ = 1.14 g cm^{-3} at 30 °C at the same temperature.

2. Medium Side Chains (R = $C_{10}H_{21}$, $C_{12}H_{25}$). These two polymers show melting points at about 70 and 95 °C, respectively, which are recognized as transitions from the solid state into a highly viscous, birefringent melt. The viscosity of this mesophase decreases to some extent upon heating but no further phase transition is observed up to 300 °C. No particular optical texture could be identified because of the strong absorption of the material and its very high viscosity.

Figure 5 shows the DSC traces of C12PCPS in subsequent heating and cooling cycles. Above room temperature two endotherms are observed: The first one at 54 °C indicates melting of locally crystallized side chain segments, which will be discussed in detail in the next section. The second broad transition with a maximum at 95 °C corresponds to the transition from the solid state into the mesophase. This mesophase is metastable when the

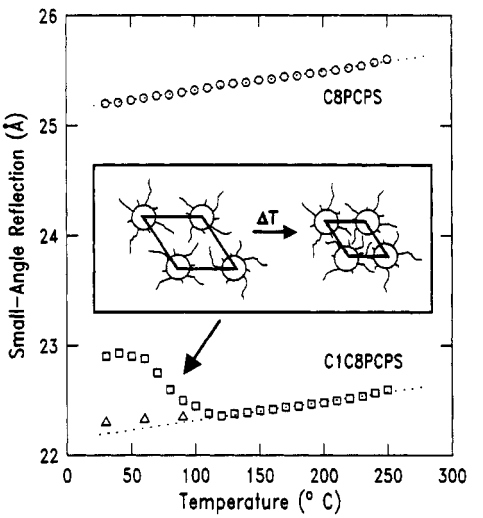

Figure 4. Temperature dependence of the d(100) spacing of C1C8PCPS measured during heating (□) and cooling (△) as compared to that of C8PCPS (○). A schematic representation of the thermal annealing process in C1C8PCPS is shown in the inset as a projection of the molecular cross-sections.

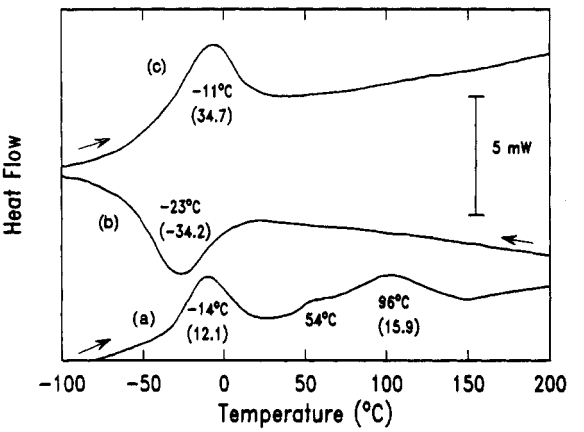

Figure 5. DSC traces of C12PCPS recorded with a heating/cooling rate of 20 °C/min: (a) first heating, (b) first cooling, and (c) second heating run. Values in parentheses denote transition enthalpies in J/g.

sample is cooled to room temperature. The only reversible transition is observed at −14 °C, which we attribute to a solid–solid transition between a low-temperature modification and the room-temperature modification.

The C10PCPS sample still shows no sign of local side chain crystallization but a reversible glass transition from the disordered side chains at −45 °C. The mesophase transition at about 70 °C is also quite broad, and the liquid-crystalline phase is metastable on subsequent cooling and heating cycles. Only within several hours did this supercooled melt transform back into the solid-state modification.

The temperature dependence of the powder X-ray diffraction pattern is quite surprising since no discontin-

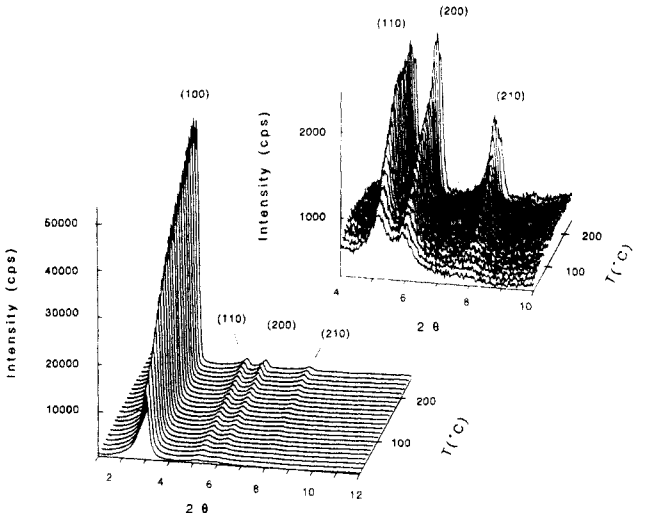

Figure 6. Temperature dependence of the X-ray diffraction pattern of C12PCPS. The inset shows a magnification of the region of the higher order reflexions.

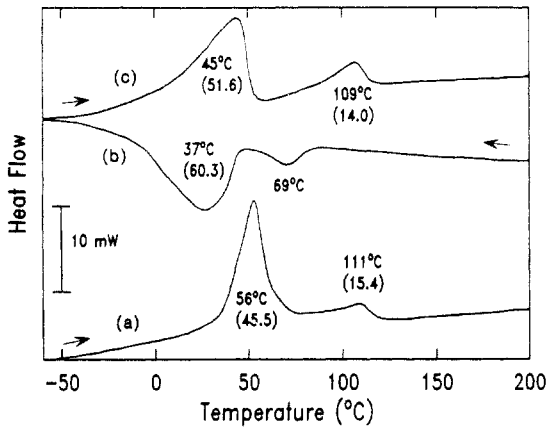

Figure 7. DSC traces of C18PCPS recorded with a heating/cooling rate of 20 °C/min: (a) first heating, (b) first cooling, and (c) second heating run. Values in parentheses denote transition enthalpies in J/g.

uous changes are observed at all, although phase transitions are obviously present. Figure 6 shows the diffraction pattern of C12PCPS between room temperature and 260 °C. Again, a highly ordered, two-dimensional hexagonal packing is observed with the orientational order increasing with temperature. In the wide-angle region again a reflection corresponding to the monomer repeat distance is observed (for d spacings see Table II), and starting with C12PCPS partial side chain crystallization at room temperature is observed for the first time. This feature will be discussed in detail in the next section. C10PCPS still has disordered side chains, as indicated by an amorphous halo located at 4.5 Å.

3. Long Side Chains (R = $C_{16}H_{33}$, $C_{18}H_{37}$). The C18PCPS polymer shows a transition at 55 °C into a highly viscous, birefringent melt. A second mesophase transition at 110 °C leads to a highly fluid but still birefringent melt. In this second liquid-crystalline phase macroscopically oriented samples can be easily prepared by slightly shearing between microscope slides. Again no typical texture is observed because of this tendency to form highly oriented monodomains. Above 180 °C a total loss of birefringence is observed in the polarizing microscope.

The DSC traces (Figure 7) indicate the same transitions, except that at about 180 °C. Note that large supercooling effects are observed during the cooling run.

The first transition can be clearly attributed to the melting of partially crystallized side chains. Figure 8 shows

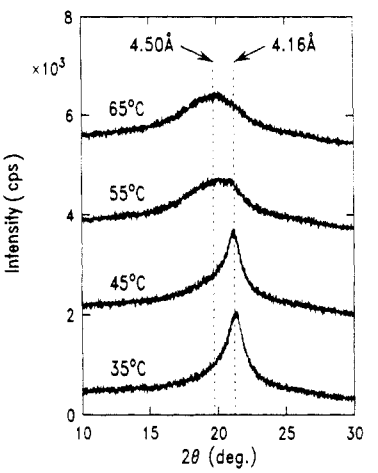

Figure 8. Wide-angle region of the X-ray diffraction pattern of C18PCPS in the temperature range of side chain melting.

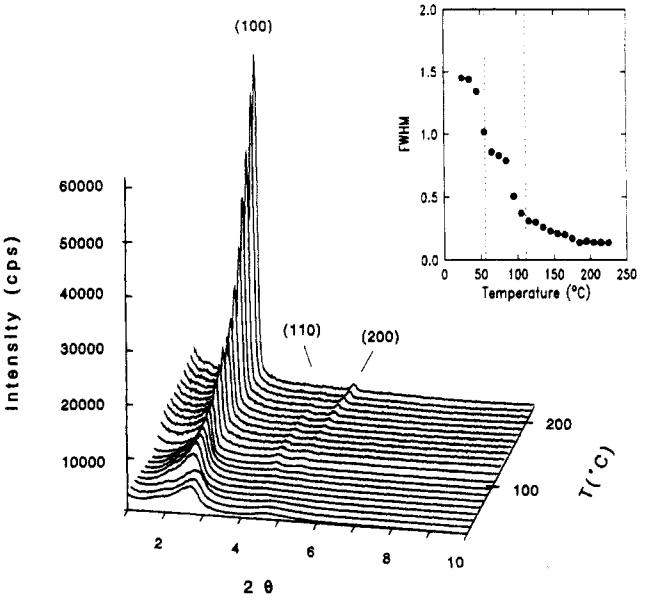

Figure 9. Temperature dependence of the X-ray diffraction patterns of C18PCPS. The inset shows the variation of the full width at half-maximum (FWHM) with temperature for the (100) reflection. Phase transition temperatures according to DSC measurements are indicated by dotted lines.

a series of wide-angle X-ray diffraction patterns in this temperature range. The Bragg peak located at 4.16 Å is transformed to an amorphous halo centered at 4.5 Å upon heating above the transition temperature. In analogy to a series of comblike polymers having n-alkyl side chains,[9] a hexagonal packing of the paraffinic moieties at room temperature is assumed. Compared to the shorter side chain polymers, it is interesting to note that side chain segments can only crystallize when they have a certain distance from the polymer main chain. About ten methylene units seem to be necessary in the present case to decouple crystallizing side chain segments from the polymer backbone. But this is of course a very general finding for polymers having alkyl side chains.[9-11]

The side chain melting also has some influence on the small-angle region of the diffraction pattern. Below the melting transition the hexagonal packing of the rigid rod macromolecules seems to be quite distorted, as indicated by rather broad reflections (Figure 9). Above the melting transition these reflections become much narrower, and the rather broad peak at $2\theta = 4.7°$ splits into the (110) and (200) reflections. Partial recrystallization of the side chains upon cooling to room temperature again leads to a

considerable broadening of the small-angle reflections. Since the lateral separation of the main chains is mainly determined by the side chain length, it is concluded that the distortion of their packing is induced by the differences in specific volume of side chain crystallites irregularly dispersed in an otherwise amorphous paraffinic matrix.

The (110) reflection slowly vanishes between 160 and 200 °C, while the (100) and (200) peaks even gain in intensity. This clearly indicates a transition from a two-dimensional hexagonal to a layered structure which at the same time is accompanied by a total loss of birefringence. It is assumed that in the two-dimensional hexagonal phase the polymer long axes orient in the plane of the sample holder in successive layers with lateral hexagonal packing, especially in the low-viscosity regime. At elevated temperature the orientational correlation between layers is lost, resulting in a pseudoisotropic (homeotropic) texture. At the same time the arrangement of layers in the plane of the sample holder is retained but not the lateral hexagonal symmetry. When the melt is cooled to 160 °C, birefringence reappears, and the X-ray experiment again shows the two-dimensional hexagonal packing of polymeric rods.

A good illustration of the layered phase is its analogy to the molecular packing in Langmuir–Blodgett films from C1C8PCPS.[8] Here layers are formed by successive transfer of monomolecular layers to a solid substrate. The molecular orientation within a layer is determined by the direction of transfer. No correlation between director axes in successive layers is observed so that pseudoisotropic layered systems can be prepared at will by varying the transfer direction continuously from layer to layer. Although individual layers cannot be manipulated in the bulk, the structures of both molecular assemblies are very similar.

C16PCPS shows a phase behavior quite similar to the higher homologue. Compared to C18PCPS the sequence of the first two transitions is reversed. The first transition is observed just below room temperature (17 °C) followed by side chain melting at 43 °C. At room temperature the material is in a highly viscous, birefringent modification which transforms to a fluid mesophase when going above the side chain melting transition. In the temperature range from 120 to 150 °C a transition to the pseudoisotropic phase is observed with a very small transition enthalpy, as indicated by DSC. X-ray measurements show a highly distorted hexagonal packing of the rigid rod macromolecules at room temperature which becomes more ordered above the melting point of the crystalline side chain segments. Starting from 125 °C the (110) reflection starts to lose intensity until at 200 °C again the layered structure is obtained.

Thermal Stability. The thermal stability of alkoxy-substituted phthalocyaninatopolysiloxanes was studied by thermogravimetric analysis (TGA), the results of which are compiled in Table III. The thermal decomposition generally starts in the range 250–300 °C with an almost quantitative side chain cleavage. A subsequent slow weight loss in the range from 500 to above 700 °C is attributed to the decomposition of the phthalocyanine core which is known to have extremely high thermal stability. When the heating rate is lowered, the temperature of maximum decomposition rate is shifted to lower temperatures while the onset of side chain cleavage remains almost constant. It is interesting to note that in the first decomposition step no significant differences are observed whether measurements are run under oxygen or nitrogen. This is a clear sign that the side chain cleavage is not an oxidative

Table III
Thermogravimetric Results for Side Chain Cleavage in Octaalkoxy-Substituted Phthalocyaninatopolysiloxanes

polymer	side chains (%)[a]	medium	heating rate (°C/min)	weight loss (%)	interval (°C)[b]	T_{max} (°C)[c]
C1C8PCPS	42.4	N_2	20	43.0	290–470	400
		O_2	20	44.7	270–530	390
		N_2	5	43.0	260–350	305
C6PCPS	50.1	N_2	20	46.9	330–630	400
		O_2	20	47.9	320–630	400
C8PCPS	57.2	N_2	20	54.8	300–500	420
C12PCPS	69.9	N_2	20	67.6	250–540	375
C16PCPS	72.7	N_2	20	73.1	250–500	420
C18PCPS	74.9	N_2	20	69.4	350–500	420
		N_2	10	64.0	280–440	370
		O_2	20	72.9	290–540	415

[a] Theoretical value as calculated from elementary composition. [b] Approximate start and end temperature of the first decomposition step. [c] Maximum of DTA curve in the decomposition range.

but rather a pyrolytic process. It is well-known that the pyrolysis of phenyl alkyl ethers occurs via β-elimination, resulting in a phenol and an olefin.[12]

Proof for the pyrolysis mechanism is obtained from infrared spectroscopy. Samples annealed in the range of 300 °C show an almost complete intensity loss in the region of the C–H modes but a remarkable increase in the O–H mode located at 3270 cm^{-1}. Such a material is not soluble even in strong aqueous base, which is a good solvent for polyphenolic structures. We anticipate that cross-linking takes place during the side chain cleavage, which is also indicated by rather broad vibration bands.

Discussion

Hexagonal-Columnar Mesophase. The characteristic property of the polymers under investigation is the hexagonal packing of rigid rod macromolecules in the solid as well as in the liquid-crystalline state. Liquid-crystalline phases of this structural type are quite uncommon in stiff chain polymers with flexible side chains. Depending on the side chain length nematic or layered mesophases are usually observed in similarly substituted fully aromatic polyesters, polyamides, and polyimides.[13–17] Watanabe and co-workers[10] have observed a phase with hexagonal symmetry in long alkyl side chain substituted poly-L-glutamates which is intermediate between the room-temperature solid modification and the cholesteric mesophase. In this material the crystallinity of side chain segments induces a layered structure of the main chains at room temperature while the intermediate hexagonal phase is built up from double-stranded α-helices.[18] X-ray reflections from the cholesteric liquid-crystalline phase of this polymer are too weak to unambiguously conclude on its packing symmetry. Very recent experimental results by Watanabe and Takashina[19] suggest that there exists an additional mesophase for this polymer in the temperature range above the cholesteric phase. The type of X-ray diffraction pattern obtained is very similar to ours. This is of course the first observation of a columnar-hexagonal phase in a thermotropic liquid-crystalline polymer. Lyotropic cholesteric mesophases from poly(benzyl L-glutamate) also show a hexagonal packing of the polymeric main chains where the (100) reflection is a function of the concentration of the binary mixture.[20] The pitch angle between molecular axes in subsequent layers along the normal is in fact so small that the hexagonal packing is retained in this cholesteric phase. Similar findings were reported for the highly concentrated lyotropic mesophase of DNA.[21]

Table IV
Phase Transition Temperatures (in °C) of Octaalkoxy-Substituted Phthalocyaninatopolysiloxanes As Determined by DSC

polymer	T_g	T_1	T_2	T_3	T_4
C1C8PCPS	-57				
C6PCPS	-55				
C8PCPS	-65				
C10PCPS	-45		70		
C12PCPS		-14	95		
C16PCPS			17	43	123
C18PCPS			56	111	160-200[a]

[a] Derived from X-ray measurements.

Furthermore some flexible polymers are known to show mesophases with hexagonal packing of the main chains, e.g. poly(bis(chlorophenoxy)phosphazene).[22] Wunderlich[23] has named this type of material "condis" crystals which in contrast to liquid and plastic crystals have both a correlation of the centers of gravity and molecular orientation but have mesomorphic properties due to conformational disorder of the polymer backbone.

The substituted phthalocyaninatopolysiloxanes investigated here belong to a structural type which Simon and co-workers[24] have named the "columnar mesophase" in analogy to discotic mesophases from low molecular weight compounds. The hexagonal packing observed in this work is different from the lamellar structure found from the oligomeric compounds investigated by the group of Simon.[24,25] Therefore the term "hexagonal-columnar mesophase" (C_h) is preferred for this structural type of liquid crystal. A tentative phase sequence based on DSC transition data can be set up as follows:

$$C_{hs_1} \underset{T_1}{\rightleftharpoons} C_{hs_2} \underset{T_2}{\rightleftharpoons} C_{hl_1} \underset{T_3}{\rightleftharpoons} C_{hl_2} \underset{T_4}{\rightleftharpoons} L$$

Here h means hexagonal, s solid, and l liquid crystalline. C_{hs_1} and C_{hs_2} are solid modifications. A transition between both is observed in C12PCPS at -14 °C. C_{hl_1} and C_{hl_2} denote the highly viscous and the fluid hexagonal-columnar mesophase. L is the high-temperature layered phase observed for the long side chain derivatives. The experimental transition temperatures according to this scheme are compiled in Table IV.

Obviously, there is no systematic correlation between transition temperatures and side chain length, which is most probably due to the fact that the polymer samples under investigation differ significantly in their molecular weights. While the C16PCPS sample is assumed to consist of rather short chain oligomers, other samples like C18PCPS or C12PCPS have weight average molecular weights in the range 200 000-300 000 and axial ratios between 6 and 15.[4] Molecular weight dependencies could not be studied at this time because of the lack of appropriate polymer samples.

Interesting to note is the analogy of the phase behavior of these polymers to that of the corresponding monomers.[26] In both cases the hexagonal-columnar mesophase is observed whether or not the disklike phthalocyanines are covalently fixed within a polymer chain. The only significant difference is the width of the mesophase, which is of course much narrower in the case of the monomers. The intermolecular forces responsible for this type of molecular packing are not fully understood at present, but recent theoretical work[27] gives evidence that it may arise at least in part from the excluded volume effect of the rigid, anisotropic particles.

Molecular Packing and Free Volume of the Side Chains. The plot of the molecular cross section of the rigid rod macromolecules as a function of the side chain length (Figure 10) demonstrates that there is no principal difference in the structure of substituted phthalocyaninatopolysiloxanes in the solid C_{hs} and in the liquid-crystalline C_{hl} phase. The cross-sectional area of a polymer molecule is calculated from the molecular diameter which in return is obtained from the d spacing of the (100) reflection according to eq 2. The unsymmetrically substituted C1C8PCPS is treated as having on average 4.5 carbon atoms per chain. d spacings from the X-ray patterns measured at 100 °C as well as rod diameters and the cross-sectional areas calculated thereof are compiled in Table II. Comparison of the data at this temperature allows for a systematic study of liquid-crystalline and nonfusible substituted phthalocyaninatopolysiloxanes.

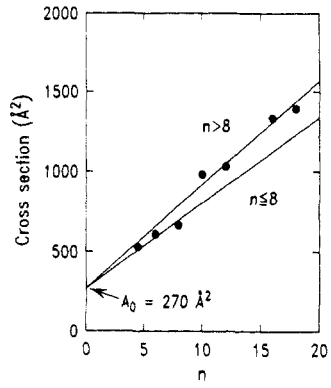

Figure 10. Cross-sectional area of the substituted phthalocyaninatopolysiloxanes as a function of the number of carbon atoms per side chain (all values at 100 °C; n = 4.5, C1C8PCPS).

In the range of experimental error the data points in Figure 10 can be approximated by a straight line each for the nonfusible ($n \leq 8$) and the liquid-crystalline derivatives ($n > 8$). Both lines have a common intercept of 270 Å^2, which is interpreted as the molecular cross-section of the phthalocyanine ring including eight oxygens. A very similar value (272 Å^2) has been found for discotic mesophases of the corresponding monomeric compounds.[26] From the slope in Figure 10 we calculate the cross-sectional area of a single methylene unit and taking into account the repeat distance along the polymer main chain (Table II), the average volume per CH_2 segment. Using an average repeat distance of 3.4 Å, we obtain at 100 °C

$$V(CH_2) = 22.7 \pm 4.8 \text{ Å}^3 \ (n \leq 8)$$

$$V(CH_2) = 27.6 \pm 3.2 \text{ Å}^3 \ (10 \leq n \leq 18)$$

Again the value for the liquid-crystalline derivatives is well in accordance with that for the discotic liquid-crystalline monomers (27.5 ± 0.6 Å^3)[26] while the result for the nonfusible polymers ($n \leq 8$) is very close to the value for the hard core volume of a CH_2 segment (23.5 Å^3) calculated by Flory and co-workers.[28] The difference of both values which is about 20% of the hard core volume is in excellent agreement with the free volume of amorphous paraffins.[28] The densities of the long side chain substituted polymers are significantly higher than those of the corresponding monomers (Table II). A value of ρ = 0.93 g cm^{-3} is calculated from the X-ray data, while the corresponding monomers show a mass density of ρ = 0.89 g cm^{-3}.[26] The densities of the nonfusible polymers are in the range of ρ = 1.10 g cm^{-3}.

Conclusions

Our investigations have shown that substituted phthalocyaninatopolysiloxanes form liquid-crystalline phases

if the side chains exceed a critical length. The common feature of all polymers is the two-dimensional hexagonal lattice which is observed in all solid and liquid-crystalline modifications. This supramolecular arrangement can be preferably compared to a nematic liquid-crystalline phase with the additional constraint of a lateral hexagonal packing. We attribute this additional structural feature to the conformational rigidity of the polymer backbone which gives these macromolecules the overall shape of circular cylinders. From the very high thermal stability of this type of packing we anticipate the molecular conformation being almost independent from temperature; e.g. the temperature coefficient of the persistence length is assumed to be rather small. This behavior has to be compared to other stiff chain polymers where a limited flexibility[6] leads to deviations from the overall rodlike structure. The typical nematic liquid-crystalline phase is a consequence of these lowered lateral constraints. These arguments are supported by the results of Krigbaum and co-workers[29] which suggest that the limited width of the nematic mesophase is determined by a considerable temperature coefficient of the persistance length.

Although the phase behavior and the type of molecular packing in alkoxy-substituted phthalocyaninatopolysiloxanes can be well understood on the basis of the rigid rod molecular conformation, a couple of questions remains open, in particular on how the observed transitions can be understood from a molecular dynamics point of view. These questions cannot be answered at the present time since more experimental data are needed, especially X-ray measurements at low temperature and from oriented samples. Solid-state NMR spectroscopy could be quite helpful in evaluating the observed phase transitions in terms of molecular dynamics of different building blocks of the molecules. In particular the study of the side chain dynamics, rotational and translational diffusion of the rods, and also rotational dynamics of the phthalocyanine units within a polymer chain are anticipated to give a better understanding of the nature of the observed transitions. These investigations are part of ongoing work in our laboratories.

Acknowledgment. The author is indebted to Prof. Dr. Gerhard Wegner for continuous support and many helpful discussions. Financial support by the Bundesministerium für Forschung und Technologie under the project "Steife Makromoleküle mit flexiblen Seitenketten" is gratefully acknowledged.

References and Notes

(1) Ballauff, M. *Angew. Chem.* **1989**, *101*, 261; *Angew. Chem., Int. Ed. Engl.* **1989**, *28*, 253.
(2) Caseri, W.; Sauer, T.; Wegner, G. *Makromol. Chem., Rapid Commun.* **1988**, *9*, 651.
(3) Sauer, T.; Caseri, W.; Wegner, G. *Macromolecules*, submitted for publication.
(4) Sauer, T.; Wegner, G. *Macromolecules* **1991**, *24*, 2240.
(5) März, K.; Ballauff, M. Unpublished results.
(6) Jung, B.; Stern, R. *Macromolecules* **1989**, *22*, 3628.
(7) Marks, T. J. *Science* **1985**, *227*, 881.
(8) Sauer, T.; Arndt, T.; Batchelder, D. N.; Kalachev, A. A.; Wegner, G. *Thin Solid Films* **1990**, *188*, 341.
(9) Plate, N. A.; Shibaev, V. P. *Comb-Shaped Polymers and Liquid Crystals*; Plenum Press: New York, 1987.
(10) Watanabe, J.; Ono, H.; Uetmasu, I.; Abe, A. *Macromolecules* **1985**, *18*, 2141.
(11) Zens, A. Dissertation, Mainz, 1989.
(12) Meerwein, H. In *Methoden der Organischen Chemie*; Thieme: Stuttgart, 1965; Vol. VI/3.
(13) Ballauff, M.; Schmidt, G. F. *Mol. Cryst. Liq. Cryst.* **1987**, *147*, 163.
(14) Majnusz, J.; Catalla, C. M.; Lenz, R. W. *Eur. Polym. J.* **1983**, *19*, 1043.
(15) Berger, K.; Ballauff, M. *Mol. Cryst. Liq. Cryst.* **1988**, *157*, 109.
(16) Wenzel, M.; Ballauff, M.; Wegner, G. *Makromol. Chem.* **1987**, *188*, 2865.
(17) Hermann-Schönherr, O.; Wendorff, J. H.; Ringsdorf, H.; Tschirner, P. *Makromol. Chem., Rapid Commun.* **1986**, *7*, 791.
(18) Watanabe, J.; Ono, H. *Macromolecules* **1986**, *19*, 1079.
(19) Watanabe, J.; Takashina, Y. *Macromolecules* **1991**, *24*, 3423.
(20) DuPre, D. B.; Samulski, E. T. In *Liquid Crystals: The Fourth State of Matter*; Saeva, F. D., Ed.; Marcel Dekker: New York, 1979.
(21) Livolant, F.; Levelut, A. M.; Doucet, J.; Benoit, J. P. *Nature* **1989**, *339*, 724.
(22) Desper, C. R.; Schneider, N. S. *Macromolecules* **1976**, *9*, 424.
(23) Wunderlich, B.; Grebowicz, J. *Adv. Polym. Sci.* **1984**, *60/61*, 1.
(24) Sirlin, C.; Bosio, L.; Simon, J. *Mol. Cryst. Liq. Cryst.* **1988**, *155*, 231.
(25) Sirlin, C.; Bosio, L.; Simon, J. *J. Chem. Soc., Chem. Commun.* **1988**, 236.
(26) Sauer, T.; Wegner, G. *Mol. Cryst. Liq. Cryst.* **1988**, *162B*, 97.
(27) Frenkel, D. *Liq. Cryst.* **1989**, *5*, 929.
(28) Flory, P. J.; Orwoll, R. A.; Vrij, A. *J. Am. Chem. Soc.* **1964**, *86*, 3507.
(29) Krigbaum, W. R.; Brelsford, G.; Ciferri, A. *Macromolecules* **1989**, *22*, 2487.